Arabian Journal of Chemistry (2020) 13, 7978–7989

King Saud University

Arabian Journal of Chemistry

www.ksu.edu.sa
www.sciencedirect.com

ORIGINAL ARTICLE

# Fabrication, characterization and X-band microwave absorption properties of PAni/$Fe_3O_4$/PVA nanofiber composites materials

**Zakiyyu Ibrahim Takai** [a,b,c,*], **Mohd Kamarulzaki Mustafa** [a,b], **Khairunnadim Ahmad Sekak** [d], **H.K. AbdulKadir** [e], **Saliza Asman** [b], **Aisha Idris** [f], **J. Mohammad** [f]

[a] *Microelectronic and Nanotechnology-Shamsuddin Research Centre (Mint-SRC), Universiti Tun Hussein Onn Malaysia (UTHM), Malaysia*
[b] *Department of Physics and Chemistry, Faculty of Applied Sciences and Technology, Universiti Tun Hussein Onn Malaysia, Pagoh Educational Hub, 86400 Muar, Johor, Malaysia*
[c] *Department of Physics Faculty of Science Yusuf Maitama Sule University, Kano, Nigeria*
[d] *Faculty of Applied Sciences, Universiti Teknologi Mara (UiTM), 40450 Shah Alam, Selangor, Malaysia*
[e] *Department of Chemical & Petrochemical Engineering, College of Engineering, University of Anbar, Ramadi, Iraq*
[f] *Faculty of Science, Federal University Dutse, Jigawa State, Nigeria*

Received 15 November 2019; accepted 14 September 2020
Available online 29 September 2020

**KEYWORDS**

Microwave absorption properties;
Electrospinning;
Nanofiber composites;
Morphology

**Abstract** This work presents a study of microwave absorption properties of PAni/$Fe_3O_4$/PVA nanofiber composites with different ratio of $Fe_3O_4$ nanoparticles. The morphology of the composites nanofibers study by Field Emission Scanning Electron Microscopes (FESEM) and Transmission Electron Microscope (TEM) showed that the low content of $Fe_3O_4$ nanoparticles presence in the composites nanofibers indicates very much uniform surface, in the composites nanofiber without many bends, but some bends develop at higher content of $Fe_3O_4$ nanoparticles as indicated in the TEM image. Image-J software was used to further investigate the diameter of the composites nanofiber and found to be in the range of 152 to 195 nm. The nanofiber composites show excellent electric and magnetic properties and therefore vary with the addition of $Fe_3O_4$ nanoparticles in the composites nanofiber. In addition the PAni/$Fe_3O_4$/PVA composites nanofibers were further characterized by X-ray diffraction spectra (XRD) and Four Transformation infrared spectra (FTIR). The XRD pattern shows the presence of PAni nanotubes containing $Fe_3O_4$ nanoparticles by indi-

* Corresponding author.
E-mail address: Zitakai21@gmail.com (Z. Ibrahim Takai).
Peer review under responsibility of King Saud University.

Production and hosting by Elsevier

https://doi.org/10.1016/j.arabjc.2020.09.027

cating peaks at 23.4$^0$ and 35.43$^0$ which was further supported by FTIR analysis. Microwave vector network analyzers (MVNA) were used to estimate the microwave absorption properties of the composites nanofibers. The absorption parameters was found to be −6.4 dB at 12.9 GHz within the range of X-band microwave absorption frequency, this reflection loss is attributed to the multiple absorption mechanisms as a result of the improved of impedance matching between dielectric and magnetic loss of the absorbent materials demonstrating that these materials can be used as protective material for electromagnetic radiation.



## 1. Introduction

Due to the popularity of electrical and electronic equipment, electromagnetic pollution has increased and has become a serious problem in modern society. The electromagnetic interference (EMI) can cause various problems such as energy, resource, mortality and human morbidity (Guo et al., 2009; Qiu and Qiu, 2015). A kind of shielding mechanism has been proposed base on nanofibrous composites prepared by electrospinning method. Electrospinning is an exceptional technique for processing a viscous solution or melt into continuous nanofibers with a uniform diameter of 500 nm or less for microwave absorption (Mohammad et al., 1996; Matthews et al., 2002), its simplest and straightforward techniques that can produce continuous polymeric nanofibrous composites through the action of an external electric field imposed on the polymer solution or melt (Sultan Lipol and Moshiur Rahman, 2016). Owing to their large surface area to volume ratio and unique nanometre scale architecture, the extraordinary application is being explored in many fields, such as absorption, surface reflection and multiple reflections (Park et al., 2014). In general, after the molecular parameter and process parameter are provided, almost all the soluble polymers can be processed into nanofiber by an electrospinning method, these include polyaniline, polypyrrole and polythiophene, while blended some water-soluble polymers such as poly(ethylene) and poly(vinyl alcohol) etc.

The electromagnetic absorbing performance of any materials depends on the intrinsic and extrinsic electromagnetic properties of materials. The intrinsic electromagnetic properties of materials include electric, magnetic, complex permittivity and permeability. The extrinsic properties consist of thickness, morphology, working frequency and structure of materials (Takai et al., 2018). Some inorganic materials such as nickel and cobalt possess large electric and magnetic loss and usually cannot be used as electromagnetic wave absorbers (Song, 2016). On the other hand, organic and inorganic materials such as polyaniline and magnetite nanoparticles possess low densities, easy processability and high electromagnetic properties, the polymeric substance could overcome the above-mentioned restriction (Feng, 2016; Song, 2017).

Polyaniline (PAni) is one of the outstanding conducting polymers due to its extraordinary properties such as high electrical conductivity, stable in the environment and easy preparation method which make it eligible in many applications (Shambharkar and Umare, 2010; Yang et al., 2009). Recently, various approached have been developed to achieve 1D nanostructure of PAni this includes nanotube, nanowire and nanorod due to their unique potential application as microwave absorbent material (de Araújo, 2010; Tayebi et al., 2016). However, it remains a great challenge to fabricate PAni's nanofibers through electrospinning due to nature of its insolubility in many solvents. To overcome this problem, mixtures of PAni with other spinnable polymers were tested (Singh, 2012; Farias-Mancilla et al., 2016).

The magnetite ($Fe_3O_4$) nanoparticles have been studied extensively owing to their exceptional magnetic properties, their magnetic feature has found widespread use in the application as diverse as environmental remediation, drug delivery release, magnetic recording media and magnetic resonance imaging and microwave absorber (Chattopadhyay et al., 2015).

In the past few decades, multifunctional composites materials gain considerable attention due to their exceptional properties and potentials in many applications in the field of science and engineering, the polymeric nanofibrous composites are an exciting new category of materials used for numerous applications particularly for microwave absorption technology (Kizildag et al., 2013).

In the current research, PAni/$Fe_3O_4$/PVA composites nanofibers were prepared by electrospinning technique to study the EM shielding properties of the composites nanofibers. The microwave absorption performance of the prepared composites was compared with X-band microwave absorption frequency. Furthermore, the electric and magnetic behaviour of the composites nanofibers were investigated by four-point probe and VSM, in addition, the morphology and structure of the composites were also evaluated using FESEM, XRD and FTIR.

## 2. Materials

In the current research, the $Fe_3O_4$ nanoparticles modified aniline dimer-COOH was prepared through co-precipitation method, further, PAni/$Fe_3O_4$ nanocomposites were synthesized by assisted ultrasonic dispersion method. However, the PAni/$Fe_3O_4$ composites were father blended in poly (vinyl) alcohol (PVA) to obtained PAni/$Fe_3O_4$/PVA nanocomposites solution via sol–gel for electrospinning method. All the chemical were used as received, which include Ammonium hydroxide ($NH_4OH$) (Sigma Aldrich), $FeCl_2$ (Sigma Aldrich), $FeCl_3$ (Sigma Aldrich), Succinic anhydride (Sigma Aldrich), N-phenyl-1,4-phenylenediamine (Sigma Aldrich), dichloromethane $CH_2Cl_2$ (Sigma Aldrich) and Diethyl ether, ammonium peroxidisulfate $(NH_4)_2S_2O_8$ (Sigma Aldrich), aniline ($C_6H_5NH_2$ R & M chemicals), Dimethyl sulfoxide (DMSO) (Sigma Aldrich), polyvinyl alcohol (Mw 89–90) (Sigma Aldrich), and Sulphuric acid $H_3PO_4$ (Sigma Aldrich). This above chemical could use in the production of nanofiber textile materials for X-band microwave absorption application.

### 2.1. Aniline dimer-COOH preparation

The preparation aniline dimer-COOH was carryout under 200-ml round bottom flask using mechanical stirrer. 0.721 g of N-phenyl-1, 4-phenylenediamine and 3.5 g of succinic anhydride were dissolved into a 30 ml of dichloromethane ($CH_2Cl_2$) under mechanical stirrer for a period of 5 h. As the reaction attend some period of time, the white grey precipitate was achieved, finally, the precipitate was washed, filtered and then dried in the vacuum for 24 h.

### 2.2. Synthesis of magnetite ($Fe_3O_4$) nanoparticles

The magnetite ($Fe_3O_4$) nanoparticles were prepared through a chemical co-precipitation method. 5.4 g of $FeCl_3$ and 3.18 g of $FeCl_2$ were added into 100 ml of deionized distilled water under vigorous magnetic stirrer at 50 °C for 1 h. 10 ml of ammonium ($NH_4$) was added subsequently followed by addition of aniline dimer-COOH in 5 ml of acetone. The solution was allowed to proceed for a period of 1.5 h obtained stable water-based suspension. The precipitated was allowed to cool to room temperature and washed with water and ethanol and then dried in the vacuum for 12 h at 60 °C.

### 2.3. Synthesis of PAni/$Fe_3O_4$ nanocomposites

Ultrasonic dispersion method was employed to prepare PAni/$Fe_3O_4$ nanocomposites as explained in our previous work (Takai et al., 2018). Some quantity (0.2 ml) of aniline monomer was dispersed in 5 ml of $H_3PO_4$ in 10 ml of distilled water under ultrasonic disperser, then $Fe_3O_4$ nanoparticles at different weight ratio (5, 10, 15, 20, 25 wt%) disperse in the above solution to obtained aniline/$Fe_3O_4$ emulsion at ambient temperature. Separately 0.46 g of APS in 5 ml of $H_3PO_4$ disperse in 15 ml of distilled water and then added to the above solution dropwise and the reaction maintained under ultrasonic disperser for 4 h to the obtained suspension of Polyaniline containing modified $Fe_3O_4$ nanoparticles. Therefore, the suspension was repeatedly washed different solvent such as ethanol and acetone in order to obtained pure PAni/$Fe_3O_4$ nanocomposites and dried at room temperature for 12 h.

### 2.4. Electrospinning solution

As synthesized PAni/$Fe_3O_4$ nanocomposites were dispersed in 15 ml of Dimethyl sulfoxide (DMSO) under vigorous magnetic stirring process for a period of 1.5 h at ambient temperature to achieve a homogeneous solution of polyaniline contain a different weight ratio of $Fe_3O_4$ nanoparticles. Then 10% w/v of polyvinyl alcohol (PVA) was dissolved in 20 ml of distilled water under stirrer throughout the night to the obtained thick solution of PVA, furthermore, the solution of PAni/$Fe_3O_4$ nanocomposites in DMSO was further blended in the thick PVA solution to achieved electrospinning solution.

### 2.5. Electrospinning setup

During electrospinning techniques, traditional electrospinning apparatus was used to fabricate PAni/$Fe_3O_4$/PVA nanofibers composites, 10 ml solution of PAni/$Fe_3O_4$/PVA composites were loaded in the syringe and subsequently pump through the round head needle of the electrospinning apparatus. The DC power supply was connected across the needle and rotating collector, the flow of polymer solution was controlled using a syringe pump, while tip to collector distance was also recorded. Therefore, the uniformly deposited nanofibers were obtained and then dried in vacuum for 1 h at 30 °C, single nozzle schematic illustration of the electrospinning apparatus is shown in Fig. 1.

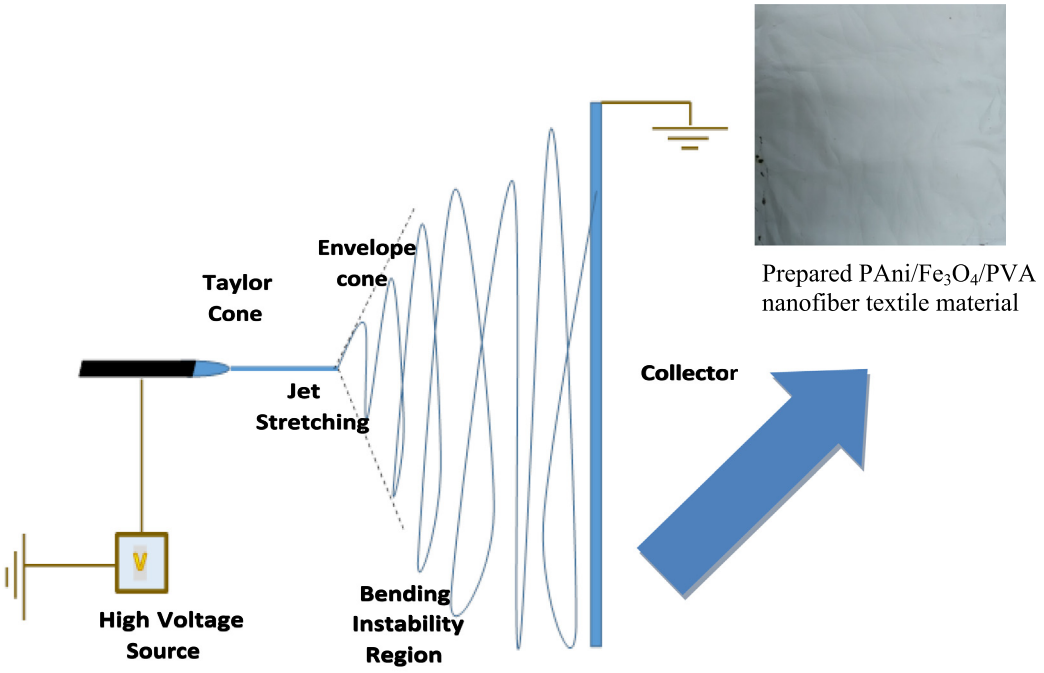


**Fig. 1** Schematic illustration of the electrospinning method.

### 2.6. Characterization

The morphologies of PAni/$Fe_3O_4$/PVA nanofiber composites contain different level of $Fe_3O_4$ nanoparticles were investigated by Field Emission Scanning Electron Microscopes (FESEM) (JEOL JSM-7600F). The average diameter of the nanofiber was measured from FESEM images using Image J software (National Institute of Health, USA) from 100 fibres. Transmission Electron Microscope (TEM) (FeiTecnia G2-STWIN) was used to study the internal morphology of the composite nanofibers. The phase structure of the PAni/$Fe_3O_4$/PVA nanofiber composites was estimated using X-ray diffraction analysis (XRD) at a radiation wavelength of ($\lambda$ = 0.154 nm) on X-pert pro MPD diffractometer using Cu K$\alpha$ radiation. Fourier Transformation infrared spectroscopy (FTIR) was used to record the molecular structure and functional group of PAni/$Fe_3O_4$/PVA nanofiber composites samples (Nicolet 560 FTIR spectrometer). The microwave absorption of all sample was investigated by HP Vector Network Analyzer (Model 851ES) in the frequency range of 2–13 GHz at room temperature. The entire samples were cut into a rectangular shape (22.86 × 10.16 mm) to fit in rectangular wave-guide of X-band. The conductivity of PAni/$Fe_3O_4$/PVA nanofiber composites containing a different weight ratio of $Fe_3O_4$ nanoparticles (5, 10, 15, 20, 25%wt) was measured by standard four-point probe apparatus (Guangzhou semiconductor materials) at ambient temperature. The magnetic properties of the magnetite nanoparticles, as well as PAni/$Fe_3O_4$/PVA nanofiber composites, were measured using vibrating sample magnetometer (VSM) JDM-1 in the magnetic field of 10KOe at room temperature.

## 3. Result and discussion

### 3.1. Morphology analysis

The morphology of the prepared nanofibers composites textiles materials recorded on Field Emission Scanning Electron Microscopes (FESEM) and Transmission Electron Microscope (TEM) is showed in Fig. 2. The PAni/$Fe_3O_4$/PVA nanofiber composites solution were loaded on 10 ml syringe and the electrospinning parameters were set at 16 kV volt, flow rate 0.3 ml/h and 10 cm tips to the needle to collector distance. The obtained results evidently revealed that the magnetite nanoparticles were spread all over the composites nanofibers materials (Kizildag et al., 2013; Liu et al., 2013). Furthermore, the magnetite nanoparticles was partially agglomerated on the surface of the nanofiber composites materials, it was further confirmed from the TEM results the primary accumulation of magnetite nanoparticles on the nanofiber surface was effectively prevented. The PAni/$Fe_3O_4$/PVA nanofiber composites size was found to increase with addition of $Fe_3O_4$ nanoparticles in the composites nanofibers as shown by TEM image, in order to confirm the actual diameter of the composites nanofibers, image-J computer software are used in our research and the result revealed as inserted in the Fig. 2, the composites nanofibers was found to be snowballing with addition of $Fe_3O_4$ nanoparticles in the composites nanofibers. The average diameter of the composites nanofibers were found to be in the range of 67 to 195 nm which is almost similar to that obtained using FESEM particles analysis. Moreover, embedding more number of $Fe_3O_4$ nanoparticles usually lower the solution viscosity and therefore the electrospinning of these may be hinder due to low viscosity as the solution would likely to spray on the collector instate of spinning, these lead to the formation of nanofiber with different diameter. Therefore, these ascribed to the facts that the addition of nanoparticles leads to the formation of more droplet on the collector, but in rare cases droplet are enforce to squish due to electrostatic force which result in the formation of nanofiber with different diameter, while some part of the nanofiber travel directly of the collector cover with aluminum foil paper which causing grip of the composites nanofibers textiles materials (Shahi et al., 2011; Hasrul et al., 2015).

The process of electrospinning was theoretically influenced with the amplification of the electric field which leads the jet to accelerate more and become stronger with the influence of repulsive force (Ngadiman et al., 2017). The diameter of the composites nanofiber has increased significantly over the increase of electrospinning applied volt. The size of the composites nanofibers has been influenced by different loading of $Fe_3O_4$ nanoparticles, these variations of the diameter were also ascribed by electrospinning applied volt to the extent that the electrospinning voltage makes the Taylor cone to be less stable to toward the formation of homogeneous composites nanofibers materials (Ngadiman et al., 2017; Song, 2017). The optimum electrospinning applied volts was found to be 16 kV as the electrospinning composites nanofibers are mostly homogeneous with almost 90% are in the range of 152–195 nm as revealed in Fig. 2.

### 3.2. Crystalline phase analysis for PVA, PAni/PVA and PAni/$Fe_3O_4$/PVA nanofibers composites

It's well known that most polymers are not entirely crystal because the chains or parts of the chains have no order to the arrangement of their chain, therefore a polymer has two phases, crystalline portion and the amorphous portion (Song, 2017). The existence of the amorphous portion leads to the appearance of characteristic amorphous halos in a different pattern. The crystalline phase of PVA, PAni/PVA and PAni/$Fe_3O_4$/PVA composites nanofibers textile are determined by X-ray diffraction spectra (XRD) and the results are shown in Figs. 3 & 4 (10 ml spinning solution at 16 kV spinning voltage).

Generally, the XRD pattern of all the samples of PAni/$Fe_3O_4$/PVA composites nanofibers textile with different contents of $Fe_3O_4$ nanoparticles shows similar XRD diffraction pattern due to the fact that the phase structure of the composites nanofiber textile materials didn't change with the influence of electrospinning parameters.

Furthermore, Fig. 3 record the existence of PVA and PAni/PVA nanofibers composites textile on X-ray diffractometry from 20 to 90° and 10 to 90° for PAni/$Fe_3O_4$/PVA composites nanofibers textile as seen in Figures (3 & 4). The phase structure that is identical to the Joint Committee on Powder Diffraction Standards file (JCPDS: 98–5970) with phase appear for each composite. The X-ray diffraction patterns of Fig. 3 clearly shows that the PVA and PAni/PVA composites nanofibers textile indicate amorphous behaviour with minor peaks at 2$\theta$ = 24.13°, 32.13°, 37.14° and 54.33° which represent the characteristic of doped PAni in the matrix. The peak

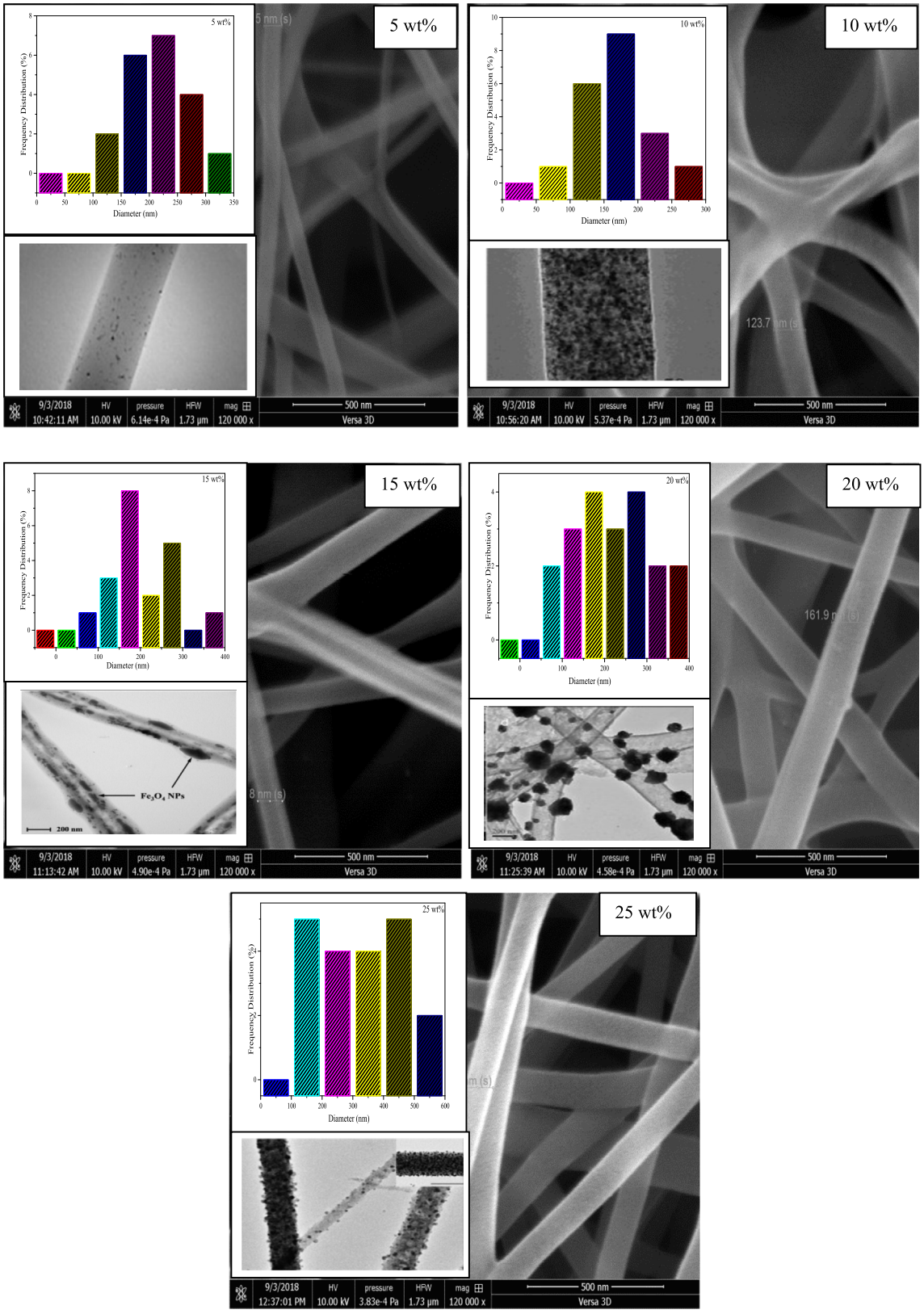


**Fig. 2** FESEM image of PAni/$Fe_3O_4$/PVA nanofibers composites with different content of $Fe_3O_4$ nanoparticles spinning with 10 ml (16 kV, 0.3 m/h and 10 cm) with image-J software result inserted in the FEWEM image.

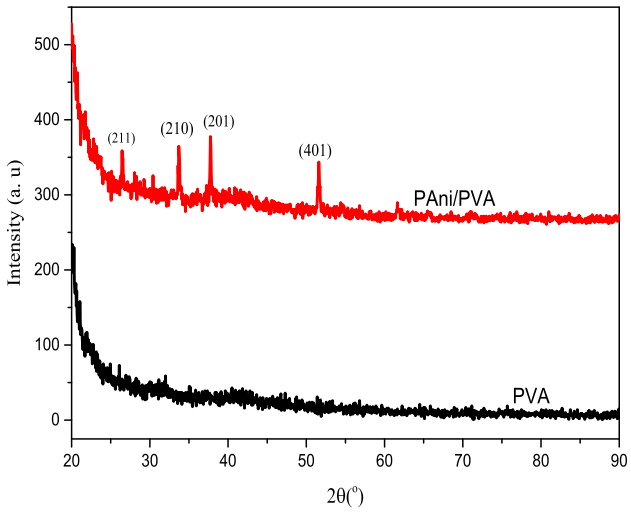


**Fig. 3** XRD plot of PVA and PAni/PVA composites nanofibers textile prepared at 0.3 ml/h, 10 cm tips to collector distance.

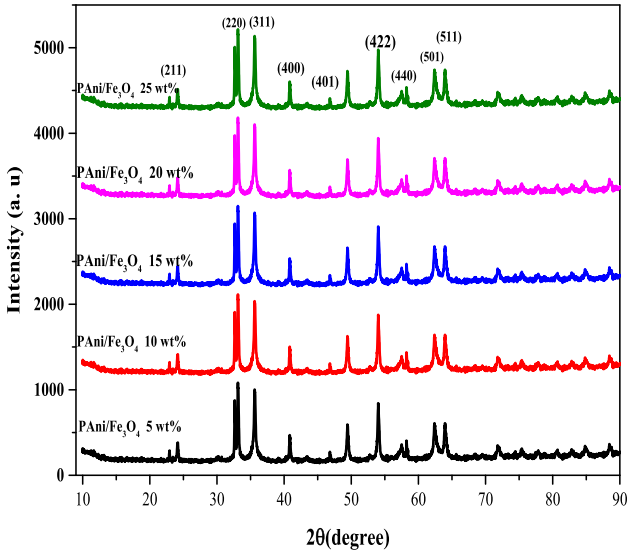


**Fig. 4** XRD plot of 10 ml solution of PAni/$Fe_3O_4$/PVA nanofibers composites prepared at 0.3 ml/h, 10 cm tips to collector distance with different content $Fe_3O_4$ nanoparticles.

at 24.13° is attributed to the periodicity parallel and perpendicular of the polymer chain direction of PAni matrix (Song, 2017; Yu et al., 2016). Additionally, the XRD pattern of the entire sample of PAni/$Fe_3O_4$/PVA nanofiber composites with different loadings of $Fe_3O_4$ nanoparticles showed an X-ray diffraction pattern similar to 10 to 90°, and the phase structure was identical to the Joint Committee on Powder Diffraction Standard file (JCPDS: 98–3860) which indicate the phase of each composite. The X-ray diffraction pattern clearly evaluates that all PAni composites exhibit amorphous behaviour with a small peak at 2θ = 24.13°, which represents the characteristics of PAni doped in the matrix (Yu et al., 2016; Quan et al., 2017).

The XRD patterns of PAni/$Fe_3O_4$/PVA composite nanofibers show their amorphous properties under different amounts of $Fe_3O_4$ nanoparticles (5, 10, 15, 20, 25 wt%). This is attributable to the higher content of PAni and PVA in the nanofibers composite, and the XRD results obtained in this study are consistent with those acquired by the other group (Li, 2018; Quan, 2018). In addition, the entire PAni/$Fe_3O_4$/PVA composite nanofibers show that PVA is present by indicating the peak at 2θ = 23.2°, also by the presence of $Fe_3O_4$ was confirm by assigned the peak at 2θ = 32.94°, 35.63°, 43.33°, 57.39°, 58.15°, 62.23°, 63.93° and 71.9° (Quan, 2018).

Therefore, it can be considered that the addition of magnetic materials ($Fe_3O_4$ nanoparticles) does not affect the chemical structure of PAni/$Fe_3O_4$/PVA nanofibers composite, as all PAni/$Fe_3O_4$/PVA composite nanofibers show almost the same FTIR and XRD spectrum. In addition, no characteristic diffraction peaks of any other impurities were detected. XRD analysis of PAni/$Fe_3O_4$/PVA composite nanofibers showed that the composite nanofibers contained $Fe_3O_4$ nanoparticles, as shown in Fig. 4. However, due to the encapsulation of PAni, the relative intensity is reduced compared to the pure $Fe_3O_4$ nanoparticle peak (Quan, 2018; Estevez, 2018)

### *3.3. Chemical bonding analysis for PVA, PAni/PVA and PAni/$Fe_3O_4$/PVA nanofibers composites*

FTIR analysis were used to investigate the synthesized PVA, PAni/PVA and PAni/$Fe_3O_4$/PVA composites nanofibers textile and also to understand the existence of surface functional groups in metal interactions with polymers. Figs. 5 & 6 represents the FT-IR spectra of PVA, PAni/PVA and PAni/$Fe_3O_4$/PVA composites nanofibers textile material spinning at different parameters such as flow rate, applied voltage and tip to collector distance respectively. A weak intense peak was identified at 3436 $cm^{-1}$, 3332 $cm^{-1}$, 2967 $cm^{-1}$ and 2796 $cm^{-1}$ correspond to the O–H stretching vibrations in PVA and N-H vibrations stretching in the PAni/PVA composites nanofibers textile reveal in Fig. 5. The bands appear at 1762 $cm^{-1}$, 1498 $cm^{-1}$, 1324 $cm^{-1}$ and 1234 $cm^{-1}$ occur in all the IR spectra of PVA and PAni/PVA composites nanofibers textile are due to C–H stretching and free N–H stretching vibrations and the band at 826 $cm^{-1}$, 783 $cm^{-1}$ and 642 $cm^{-1}$ are the derives of H, C,O stretching (Estevez, 2018). In addition, the bands from 1480 to 1280 $cm^{-1}$ reveal the C–O symmetric and C = O stretching vibrations. Furthermore, in the IR spectra of PVA and PAni/PVA nanofibers textile, some peaks were observed at 510 $cm^{-1}$ was due to vibrating stretching of C-H groups which appears in PAni and PVA particles (Wang, 2018). Furthermore, present of peaks in a range of 1400 to 800 $cm^{-1}$ could be attributed to the methyl group vibration and straighten that is usually present in the PAni and PVA tube which can easily signify the loss of water molecule and scission of the methyl group (Ni et al., 2010).

To further understand the chemical bonding analysis of PAni/$Fe_3O_4$/PVA nanofibers composite, FTIR spectroscopy was performed to determine the molecular structure and chemical bonding of PAni/$Fe_3O_4$/PVA composite nanofiber materials, 10 ml 16 kV, 10 cm and 0.3 ml/h electrospinning parameters are shown in Fig. 6. However, the infrared spectra of PAni/$Fe_3O_4$/PVA composite nanofibers indicate that these polymers are more likely to interact with magnetic nanoparticles. The FTIR analysis of composite nanofibers shows that the absorption band stretched at 3462 $cm^{-1}$. There is slightly decreased and widened of the band at, 3431 $cm^{-1}$, 3372 $cm^{-1}$ and 3275 $cm^{-1}$ are due to vibration stretching

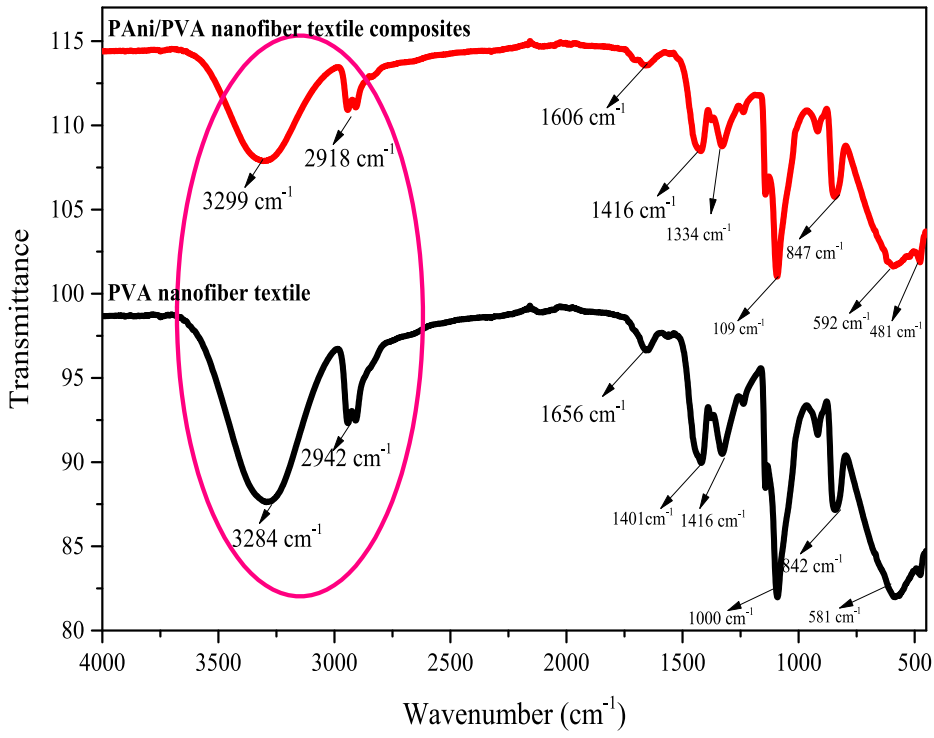


**Fig. 5** FTIR spectra of PVA, PAni/PVA nanofibers textile composites spinning at 10 ml, 0.3 ml/h and 10 cm tips to collector distance.

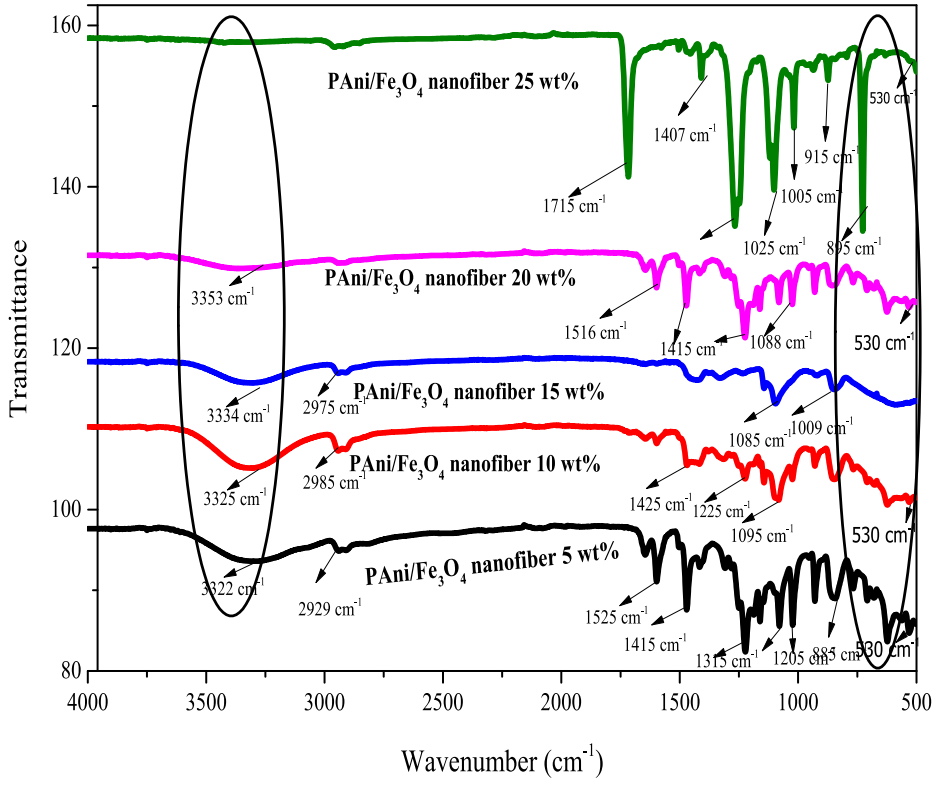


**Fig. 6** FTIR spectra of PAni/$Fe_3O_4$/PVA composites nanofibers spinning at 16 kV, 0.3 ml/h and 10 ml.

–NH groups, sudden disappearance of peaks in PAni/$Fe_3O_4$/PVA nanofibers composites containing 25 wt% $Fe_3O_4$ nanoparticles in textile materials clearly shows higher interaction of nanoparticles with nitrogen, hydrogen, carbon and oxygen atoms in the PAni and PVA chains (Wang, 2018; Ni et al., 2010).

Furthermore, due to the bond formation of the $Fe_3O_4$ nanoparticles with the O and H atoms and the disappearance of the bond, the decrease in the strength and width of the bond at 1672 $cm^{-1}$ , 1634 $cm^{-1}$ , 1521 $cm^{-1}$ indicates the decoupling between the OH and N-H bonds, in the PAni/$Fe_3O_4$/PVA nanofibers composite textile samples containing 15 and 20 wt % $Fe_3O_4$ nanoparticles were also observed at 1483 $cm^{-1}$ and also showed chemical bonding of $Fe_3O_4$ nanoparticles to PAni and PVA chain molecules (Xu et al., 2018; Ni, 2010). The change in bond strength occurred at 1490 $cm^{-1}$, 14747 $cm^{-1}$, 1062 $cm^{-1}$, 1031 $cm^{-1}$, 893 $cm^{-1}$, 784 $cm^{-1}$ and 693 $cm^{-1}$ also indicating their interaction. The main PAni matrix was doped with $Fe_3O_4$ nanoparticles, and some peaks were observed at the lowest wave number of 510 $cm^{-1}$ and 571 $cm^{-1}$, indicating the presence of $Fe_3O_4$ nanoparticles in the PAni/$Fe_3O_4$/PVA nanofibers composite textile (Ma et al., 2017).

### 3.4. Microwave absorption study

In order to investigate the microwave absorption ability of PAni/$Fe_3O_4$/PVA nanofiber composites, MVNA was employed to reveal the microwave absorption properties of the synthesized sample using the waveguide technique. Some parameter such as reflection loss (RL), relative permeability and permittivity at a given frequency as well as thickness layer in accordance with transmission line theory was calculated using the equation summarized below.

$$Z_{in} = Z_o\sqrt{\frac{\mu_r}{\varepsilon_r}}\tanh\left[j\left(\frac{2\pi fd}{c}\right)\sqrt{\mu_r\varepsilon_r}\right] \quad (1)$$

$$Z_0 = \sqrt{\frac{\mu_0}{\varepsilon_0}} = 120\pi \quad (2)$$

$$RL(dB) = 20\log_{10}\left|\frac{Z_{in} - Z_0}{Z_{in} + Z_0}\right| \quad (3)$$

Here f is the microwave frequency, C in ($m^{-1}$) is the speed of light, d in (mm) is the thickness of the absorber, $Z_0$ in (Ω) is the impedance of the air and $Z_{in}$ in (Ω) is the input impedance of the absorber. However, the relative complex permittivity and relative complex permeability were recorded using microwave vector network analyzer, at a certain frequency in rang of 2–13 GHz. Therefore, considering the absorber thickness as one of the major parameter (1.0 mm, 1.5 mm, 2.0 mm, 2.5 mm and 3.0 mm) that influences the position and intensity of the microwave frequency at reflection loss (RL) as this thickness was increase with addition of $Fe_3O_4$ nanoparticles in the composites nanofibers sample. The X-band microwave absorption study was found to be in range of 8.2–12.4 GHz, which is quite significant for commercial and many electronic application including maritime radio navigation, weather radar, Doppler, telephone microwave relay system and TV picture transmission (Liu et al., 2015; Zhang, 2017; Mohammed, 2019; Vyas et al., 2017).

The frequency dependency of the microwave absorbing properties of PAni/$Fe_3O_4$/PVA nanofiber composites is shown in Fig. 7. The RL of the composites nanofiber was calculated using equation (1), 2 and 3, while the reflection loss (RL) of the composites nanofiber contain (5–25 wt%) of $Fe_3O_4$ nanoparticles was observed and reported accordingly. The first reflection loss (RL) was revealed on the composites nanofiber

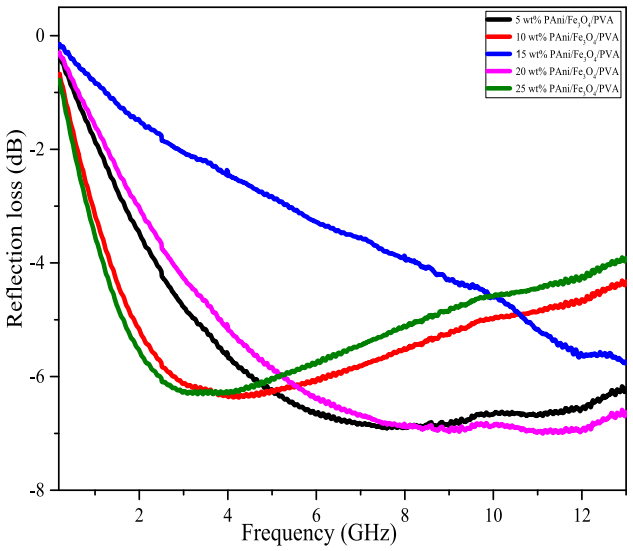


**Fig. 7** Reflection loss study for PAni/$Fe_3O_4$/PVA nanofiber composites with different content of $Fe_3O_4$ nanoparticles.

contains 10 and 25 wt% of $Fe_3O_4$ nanoparticles at −6.4 dB and −6.3 dB while the frequency was 4.2 GHz and 3.5 GHz for 10 and 25 wt% of $Fe_3O_4$ nanoparticles content respectively. The second loss of the composites nanofiber was observed at −6.38 dB and −6.6 dB while the frequency was 12.9 GHz and 12.94 GHz respectively for nanofiber composites with 5 and 20 wt% of $Fe_3O_4$ nanoparticles loading. Suggesting that the nanofiber composites sample contain (5 and 20 wt%) are more suitable for X-band microwave absorption materials (Park et al., 2016; Take et al., 2014), while the composites nanofiber sample contain 10 and 25 wt% of $Fe_3O_4$ nanoparticles are found to be within the range of S-band microwave absorbing frequency (Guo et al., 2013; Levine, 2012) that could be used for surface ship radar, weather radar, and some communication satellite (microwave device/communications, microwave oven, radio astronomy, mobile phones, wireless LAN, Zig-Bee and GPS). Compared with the conductivity results in Table 1 and Fig. 6, can observed that the composites with higher conductivities at 5 wt% nanoparticles correspond to one of the better absorbing parameters (Terrazas Reza, xxxx), this indicated that both higher and lower conductive nanofiber sample have beneficial toward improving microwave absorbing parameter of the composites nanofibers (Sulistyaningsih et al., 2015; Hariani et al., Jan 2013).

The microwave absorption study was further carryout to investigate the relative complex permeability ($\mu_r$) measured in (H/m), while relative complex permittivity ($\varepsilon_r$) in (farad $m^{-1}$) in the prepared composites nanofibers using the relation below

$$\mu_r = \mu' - j\mu'' \quad (4)$$

$$\varepsilon_r = \varepsilon' - j\varepsilon'' \quad (5)$$

The real permeability is denoted by $\mu'$ and real permittivity is $\varepsilon'$was categorise as the storage ability of electromagnetic energy, while imaginary permeability$\mu''$ is related to the magnetic loss and imaginary permittivity $\varepsilon''$ is attributed to how

**Table 1** Dependence of magnetization on the content of $Fe_3O_4$ nanoparticles in PAni/$Fe_3O_4$/PVA nanofibers composites.

| Sample No. | Content of $Fe_3O_4$ wt% | Saturated Magnetization/(emu/g) | Remnants Magnetization /(emu/g) | Coercive force /(emu/g) |
|---|---|---|---|---|
| 1 | 100 | 84.8 | 7.6 | 61.9 |
| 2 | 5 | 5.85 | 0.38 | 64.7 |
| 3 | 10 | 11.3 | 0.56 | 58.8 |
| 4 | 15 | 17 | 0.82 | 59.1 |
| 5 | 20 | 40.3 | 2.2 | 61.1 |
| 6 | 25 | 58.8 | 3.6 | 78.1 |

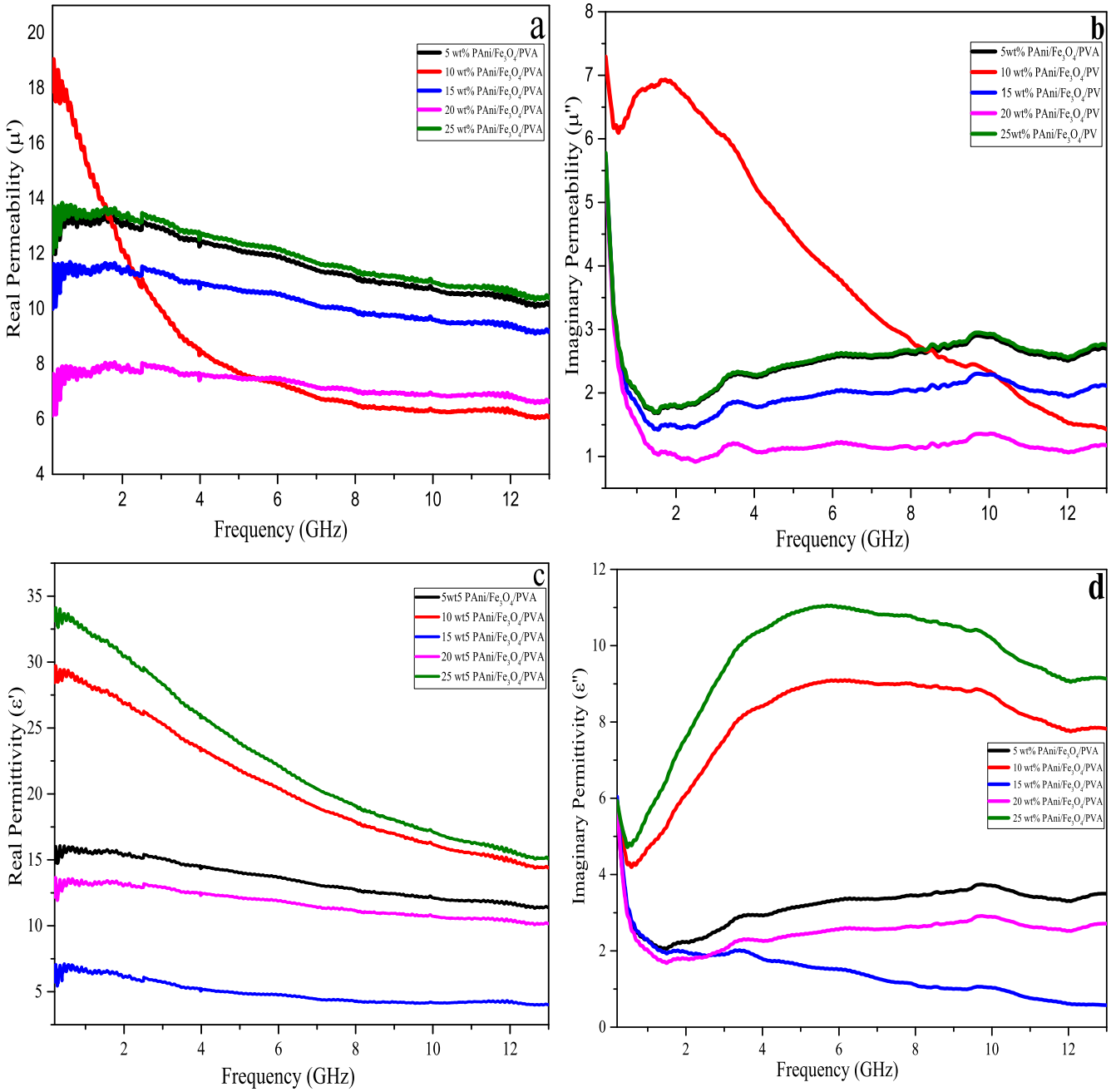


**Fig. 8** Electromagnetic parameters of PAni/$Fe_3O_4$/PVA nanofiber composites with different content of $Fe_3O_4$ nanoparticles in the range of 2–13 GHz: (a) real and (b) imaginary part of the complex permeability (c) real and (d) imaginary parts of relative permittivity.

much energy is dissipated in the absorbing medium (Bahrain et al., 2016). The curve of $\mu'$;$\mu''$ ,$\varepsilon'$, and $\varepsilon''$ for the PAni/$Fe_3O_4$/PVA nanofiberious composites at different wt% of $Fe_3O_4$ nanoparticles is shown in the Fig. 8. It is observed that the composites nanofibers contain 10 wt% of $Fe_3O_4$ nanoparticles show higher reflection coefficient values of $\mu'$ and$\mu''$ (Fig. 8 a & b) and decrease at higher frequency 2–13 GHz, which relate to the higher conductive values of the composites nanofibers, resulted from the fact that increase in the external applied electric field causes the induction charge phase of the PAni/$Fe_3O_4$/PVA nanofiber composites to lag behind the external electric field which cause the electromagnetic oscillation as well as space charge polarization to increase, this results from difference in values of $\mu'$ and$\mu''$ (Wang et al., 2014; Qiu et al., 2006; Tang, 2011). Furthermore, the $\varepsilon'$ and $\varepsilon''$ values obviously varies with variation of frequency in range of 2–13 GHz (Fig. 4 c & d), lower values of $\varepsilon'$ and $\varepsilon''$ at higher frequency result in the shortening of the interfacial impedance gap thereby decreasing the reflection coefficient of the prepared microwave absorbent materials (Cao et al., 2015). But when the ratio of $Fe_3O_4$ nanoparticles increase in the composites nanofibers (5–25 wt%) then $\varepsilon''$ and $\mu''$ values exhibit positive reflection coefficient values in the whole range, it is suggesting that the total microwave radiated can be absorb by the prepared materials (Li et al., 2013). If the values of $\varepsilon''$ and $\mu''$ are found to be negative, neither indicating that the magnetic energy is radiated nor absorption (Tayebi et al., 2016; Li et al., 2013), this is to say that the composites, are, mainly exhibit electrical losses (Singh, 2012; Li et al., 2013). Hence, the microwave absorption properties of an EM wave absorber material depend on the values of $\varepsilon'$ and $\mu'$ of the materials (Farias-Mancilla et al., 2016; Li et al., 2013). Moreover, the obtained microwave absorption could be attributed to attenuation of EM wave and impedance matching. The presence of PAni phase in the nanofiber composites has lowered the $H_c$ of the nanocomposites and also increase the dielectric properties. The conductive properties of the PAni provide the environment for improved hopping of electrons, tunnelling or free band conduction which consequently enhanced the microwave absorption properties of the nanofiber composite (Li et al., 2013). Also, the presence of residual functional groups and defects in the PAni sheets favours the absorption of microwaves (Iqbal et al., 2017). The small crystallite size of the $Fe_3O_4$ nanoparticles increase dipole polarization thereby enhancing the $\varepsilon''$ and $\mu''$ values of the nanofiber composites, the presence of multi interfaces in the nanofiber composites also serve as polarization centres which is vital for high absorption of microwaves.

### 3.5. The electrical conductivity studies

The electrical conductivities study of composites nanofibers with different contents of $Fe_3O_4$ nanoparticles were study 4-point probe apparatus and the data are shown in Fig. 9. However, the electrospinning of PAni/$Fe_3O_4$/PVA nanofibers composites was carried out, while 10 ml syringe was loaded with the electrospinning solution and spinning parameters were set at tips of the needle to collector distance 10 cm, flow rate of 0.3 ml/h and 16 kV, the variation of viscosity was attributed to the addition of $Fe_3O_4$ nanoparticles in the composites solution, the change in the electrical conductivity was

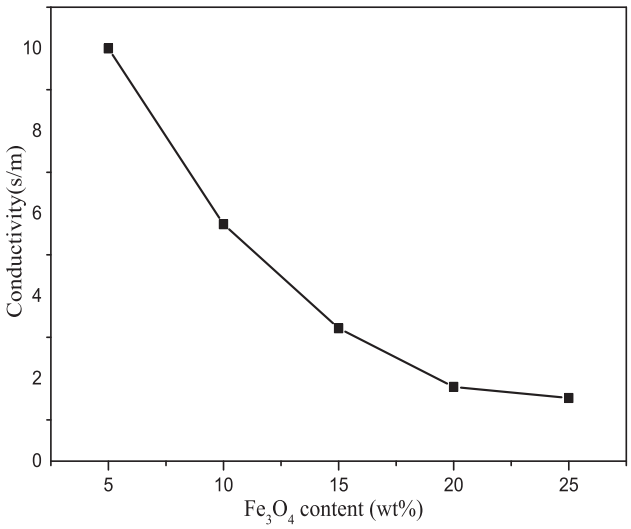


**Fig. 9** Conductivity of 10 ml solution of PAni/$Fe_3O_4$ /PVA Composites nanofibers at different $Fe_3O_4$ nanoparticles content.

ascribed to the different loading of $Fe_3O_4$ nanoparticles in the composites nanofiber which was confirm in the Fig. 9. The modified magnetite nanoparticles were found to vary the electrical conductivity due to insulating behaviour of the $Fe_3O_4$ nanoparticles in the composites. The electrical conductivity of the nanofibers composites with different loading of the magnetite nanoparticles was plotted in Fig. 9. The electrical conductivity of the nanofiber composites varies over the addition of $Fe_3O_4$ nanoparticles. Once the composites nanofiber were implanted with $Fe_3O_4$ nanoparticles, the interaction of polymers matrix with nanoparticles enhance the carrier dispersal thereby increasing the resistivity of the composites. Many factors are responsible for enhancing the carrier signals this includes electrostatic charges that usually generated during electrospinning or charges created by morphological defects or even nanoparticles themselves can play a significant role (Song, 2016; Kizildag et al., 2013; Iqbal et al., 2017). Therefore, blending magnetic ($Fe_3O_4$) nanoparticles in the conducting polymers will enhance and stabilized the association between the component, the properties of the composites nanofibers materials was influenced by the presence of magnetic nanoparticles loaded in the nanofibers composites materials (Take et al., 2014; Kim et al., 2001).

### 3.6. Magnetization studies

The saturation magnetization ($M_s$), coercive force ($H_c$) and Remnant magnetization ($M_r$) of the $Fe_3O_4$ nanoparticles and nanofibers composites were investigated using vibrating sample magnetometer (VSM) and the results were tabulated in Table 1. Several hysteresis behaviours of the prepared PAni/$Fe_3O_4$/PVA nanofibers composites materials produced with different electrospinning parameters (16 kV, 0.3 ml/h and10 cm), under the influence of the magnetic field of −10000 HOe to 10,000 HOe shows extraordinary saturation magnetization ($M_s$). Furthermore, the dependence of saturation magnetization introduces in the composites nanofibers materials recorded in Table 1. It was observed that the saturation magnetization ($M_s$), Remnant magnetization ($M_r$) and coercive force ($H_c$) were found to be $M_s$ = 84.8 emus/g $M_r$ = 7.6,

$H_c$ = 61.9. The superparamagnetic performance was observed in the absence of hysteresis behaviour in the composites nanofiber materials, the saturation magnetization ($M_s$) of the composites nanofibers was found to increase significantly due to increase of magnetic nanoparticles content (5 wt% (5.85 emu/g) to 25 wt% (58.8 emu/g)) in the composites nanofibers and therefore shows superparamagnetic performance. It is worthwhile to note that the observed magnetization of the nanofibers composites materials is considerably lower than the values recorded for the modified $Fe_3O_4$ nanoparticles. However, the interaction between *d*-orbital of the magnetite nanoparticles and the polymer matrix is ascribed to the movement of an electron with an unpaired spin in the $Fe_3O_4$ nanoparticles (Qiu et al., 2006; Medeiros, 2008). In order way round, the transfer of charges carrier on the surface of PAni and magnetite nanoparticles probably cause the variation of electron density on the surface of $Fe_3O_4$ nanoparticles thereby hindering the magnetic ability of the composites nanofibers (Lim and Choi, 2017; Keivani et al., 2010). The interphase interaction within the composites nanofibers usually varies the $M_s$ of the composites, which was found to be lower than the saturation magnetization of pure $Fe_3O_4$ nanoparticles. With controllable electrical, magnetic, and electromagnetic properties of the prepared nanofibers composites can potentially be used for X-band microwave absorption applications (Wang et al., 2018; Sun et al., 2014).

## 4. Conclusion

In summary, the morphology of the composites nanofibers was studied by Field Emission Scanning Electron Microscope (FESEM). The analysis confirms the formation of nanofiber, the Image-J software was employed to determine the diameter of the composites nanofiber and found to be in the range of 152 to 195 nm which is almost the same as the one obtained by FESEM analysis. The microwave absorption studies indicate that the dielectric properties of the composites nanofibers contribute greatly to the observation of the reflection loss. The PAni/$Fe_3O_4$/PVA composites nanofiber samples show a maximum reflection loss of −6.6 dB at 12.94 GHz as a better result of impedance matching between the magnetic and dielectric losses of the absorbent media. Furthermore the electric and magnetic properties of the composites nanofibers were also studied; it was found that the electrical conductivity of PAni/$Fe_3O_4$/PVA nanofiber composites decreased with increase of modified $Fe_3O_4$ nanoparticles in the composites nanofibers, while the saturation magnetization of PAni/$Fe_3O_4$/PVA nanofiber composites was increasing with increase of modified aniline dimer-COOH $Fe_3O_4$ nanoparticles (5.85–58.8 emus/g). In addition, the PAni/$Fe_3O_4$/PVA nanofiber composites were further characterized using FTIR and XRD, the obtained XRD result indicate the presence of $Fe_3O_4$ nanoparticles by shown the inverse cubic spinel structure, while the amorphous nature of the composites nanofiber shows the present of PAni and PVA in the composites. The chemical bonding analysis was studied using Fourier Transform Infrared Spectroscopy (FTIR). The FTIR analysis showed the disappearance of the peak in the PAni/$Fe_3O_4$ composites nanofibers sample containing 25 wt% of $Fe_3O_4$ nanoparticles clearly indicate the interaction of nanoparticles with nitrogen N, hydrogen H, carbon C, and oxygen O atoms in the PAni and PVA chain.

## Acknowledgement

The authors gratefully acknowledged the Research Management Centre (RMC), Centre for Graduate Studies (CGS) Universiti Tun Hussein Onn Malaysia (UTHM) and Universiti Teknologi Mara. 40450 Shah Alam, Selangor, Malaysia (UiTM) for their kind support and encouragement.

## References

Guo, J., Ye, X., Liu, W., Wu, Q., Shen, H., Shu, K., 2009. Preparation and characterization of poly(acrylonitrile-co-acrylic acid) nanofibrous composites with $Fe_3O_4$ magnetic nanoparticles. Mater. Lett. 63 (15), 1326–1328.

Qiu, J., Qiu, T., 2015. Fabrication and microwave absorption properties of magnetite nanoparticle- carbon nanotube-hollow carbon fibre composites. Carbon N. Y. 81 (1), 20–28.

Mohammad, F., Calvert, P.D., Billingham, N.C., 1996. Electrical and electronic properties of polyparaphenylenes. J. Phys. D. Appl. Phys. 29, 195–204.

Matthews, J.A., Wnek, G.E., Simpson, D.G., Bowlin, G.L., 2002. Electrospinning of collagen nanofibers. Biomacromolecules.

Sultan Lipol, L., Moshiur Rahman, M., 2016. Electrospinning and Electrospun Nanofibers. World J. Nano Sci. Eng. 6, 45–50.

Park, S.J., Kwon, O.S., Lee, J.E., Jang, J., Yoon, H., 2014. Conducting polymer-based nanohybrid transducers: A potential route to high sensitivity and selectivity sensors. Sensors (Switzerland).

Takai, Z.I., Mustafa, M.K., Asman, S., Ahmad, K., Jibrin, M., 2018. Preparation of Aniline Dimer-COOH Modified Magnetite ($Fe_3O_4$) Nanoparticles by Ultrasonic Dispersion Method. International Journal of Engineering & Technology 7, 185–188.

Song, W.L. et al, 2016. Strong and thermostable polymeric graphene/silica textile for lightweight practical microwave absorption composites. Carbon N. Y. 100, 109–117.

Feng, W. et al, 2016. Reduced graphene oxide decorated with in-situ growing ZnO nanocrystals: Facile synthesis and enhanced microwave absorption properties. Carbon N. Y. 108, 52–60.

Song, C. et al, 2017. Three-dimensional reduced graphene oxide foam modified with ZnO nanowires for enhanced microwave absorption properties. Carbon N. Y. 116, 50–58.

Shambharkar, B.H., Umare, S.S., 2010. Production and characterization of polyaniline/$CO_3O_4$ nanocomposite as a cathode of Zn-polyaniline battery. Mater. Sci. Eng. B Solid-State Mater. Adv. Technol. 175 (2), 120–128.

Yang, C., Li, H., Xiong, D., Cao, Z., 2009. Hollow polyaniline/$Fe_3O_4$ microsphere composites: Preparation, characterization, and applications in microwave absorption. React. Funct. Polym. 69 (2), 137–144.

de Araújo, A.C.V. et al, 2010. Synthesis, characterization and magnetic properties of polyaniline- magnetite nanocomposites. Synth. Met. 160 (7–8), 685–690.

Tayebi, H.-A., Dalirandeh, Z., Shokuhi Rad, A., Mirabi, A., Binaeian, E., 2016. Synthesis of polyaniline/$Fe_3O_4$ magnetic nanoparticles for removal of reactive red 198 from textile wastewater: kinetic, isotherm, and thermodynamic studies. Desalin. Water Treat. 57 (47), 22551–22563.

Singh, R.P., 2012. Prospects of Organic Conducting Polymer Modified Electrodes: Enzymosensors. Int. J. Electrochem. 2012, 1–14.

Farias-Mancilla, R., Elizalde-Galindo, J.T., Vigueras-Santiago, E., Hernández- Escobar, C.A., Vega- Rios, A., Zaragoza-Contreras, E. A., 2016. Synthesis and Characterization of Polyaniline/Magnetite Nanocomposite. Avestia Publ. Int. J. Theor. Appl. Nanotechnol. J. 4, pp. 1929-1248.

Chattopadhyay, S., Bajpai, O.P., Setua, D.K., 2015. A Brief Overview on Ferrite ($Fe_3O_4$) Based Polymeric Nanocomposites: Recent

Developments and Challenges. J. Res. Update. Polym. Sci. 3 (4), 184–204.

N. Kizildag, N. Ucar, H. Garmestani, and Y. Wang, "Poly (vinyl alcohol)/ Polyaniline (PVA/PANi) Conductive Nanofibers by Poly (Vinyl Alcohol)/Polyaniline (PVA/PANI) conductive," no. May 2013, 2016.

Liu, F., Ni, Q.-Q., Murakami, Y., 2013. Preparation of magnetic polyvinyl alcohol composite nanofibers with homogeneously dispersed nanoparticles and high water resistance. Text. Res. J. 83 (5), 510–518.

Shahi, M., Moghimi, A., Naderizadeh, B., Maddah, B., 2011. Electrospun PVA-PANI and PVA-PANI- $AgNO_3$composite nanofibers. Sci. Iran. 18 (6), 1327–1331.

N. Hasrul, A. Ngadiman, A. Idris, and M. Irfan, "γ -Fe2O3 nanoparticles fi lled polyvinyl alcohol as a potential biomaterial for tissue engineering scaffold," vol. 49, pp. 90–104, 2015.

Ngadiman, N.H.A., Yusof, N.M., Idris, A., Misran, E., Kurniawan, D., 2017. Development of highly porous biodegradable γ-$Fe_2O_3$/polyvinyl alcohol nanofiber mats using electrospinning process for biomedical application. Mater. Sci. Eng. C 70, 520–534.

Song, W.L. et al, 2017. A universal permittivity-attenuation evaluation diagram for accelerating design of dielectric-based microwave absorption materials: A case of graphene-based composites. Carbon N. Y 118, 86–97.

Yu, H., Wu, L., Chen, S., Wu, Q., Yang, Y., Edwards, H., 2016. Caregiving burden and gain among adult-child caregivers caring for parents with dementia in China: The partial mediating role of reciprocal filial piety. Int. Psychogeriatrics 28 (11), 1845–1855.

Quan, L., Qin, F.X., Estevez, D., Wang, H., Peng, H.X., 2017. Magnetic graphene for microwave absorbing application: Towards the lightest graphene-based absorber. Carbon N. Y 125, 630–639.

Li, Y. et al, 2018. Fe@C nanocapsules with substitutional sulfur heteroatoms in graphitic shells for improving microwave absorption at gigahertz frequencies. Carbon N. Y. 126, 372–381.

Quan, B. et al, 2018. Laminated graphene oxide-supported high-efficiency microwave absorber fabricated by an in situ growth approach. Carbon N. Y. 129, 310–320.

Estevez, D. et al, 2018. Complementary design of nano-carbon/magnetic microwire hybrid fibres for tunable microwave absorption. Carbon N. Y. 132, 486–494.

Wang, F. et al, 2018. Microwave absorption properties of 3D cross-linked Fe/C porous nanofibers prepared by electrospinning. Carbon N. Y. 134, 264–273.

Ni, S., Wang, X., Zhou, G., Yang, F., Wang, J., He, D., 2010. Designed synthesis of wide range microwave absorption $Fe_3O_4$-carbon sphere composite. J. Alloys Compd. 489 (1), 252–256.

Xu, W., Pan, Y.F., Wei, W., Wang, G.S., Qu, P., 2018. Microwave absorption enhancement and dual- nonlinear magnetic resonance of ultra-small nickel with quasi-one-dimensional nanostructure. Appl. Surf. Sci. 428, 54–60.

Ni, S. et al, 2010. Low temperature synthesis of $Fe_3O_4$ micro-spheres and its microwave absorption properties. Mater. Chem. Phys. 124 (1), 353–358.

Ma, C., Zhao, B., Dai, Q., Fan, B., Shao, G., Zhang, R., 2017. Porous structure to improve microwave absorption properties of lamellar ZnO. Adv. Powder Technol. 28 (2), 438–442.

Liu, X., Guo, H., Xie, Q., Luo, Q., Sen Wang, L., Peng, D.L., 2015. Enhanced microwave absorption properties in GHz range of $Fe_3O_4$/C composite materials. J. Alloys Compd. 649, 537–543.

Zhang, H. et al, 2017. Magnetic nanoparticle-loaded electrospun polymeric nanofibers for tissue engineering. Mater. Sci. Eng. C 73, 537–543.

Mohammed, J. et al, 2019. Lightweight SrM/CCTO/rGO nanocomposites for optoelectronics and Ku-band microwave absorption. J. Mater. Sci. Mater. Electron. 26 (2).

S. Vyas, S. Shivhare, and A. Shukla, "Polyaniline (PANI) Metal Oxide Nano Composites as a Conducting Material," vol. IV, no. Vii, pp. 86–89, 2017.

Park, C.S., Lee, C., Kwon, O.S., 2016. "Conducting Polymer-Based Nanobiosensors".

Take, S., Akbari, A., Talebi, A., Talebi, E., 2014. Synthesis and characterization of tin oxide nanoparticles via the Co-precipitation method. Mater. Sci. 32 (1), 98–101.

Guo, C., Zhou, L., Lv, J., 2013. Effects of expandable graphite and modified ammonium polyphosphate on the flame-retardant and mechanical properties of wood flour- polypropylene composites. Polym. Polym. Compos. 21 (7), 449–456.

Levine, O.M. et al, 2012. Sol-gel synthesis of 8nm magnetite ($Fe_3O_4$) nanoparticles and their magnetic properties. Superlattices Microstruct.

R. Terrazas Reza, C. A. Martínez Pérez, A. Martínez Martínez, and P. E. García- Casillas, "Magnetite Particle Size Dependence on the Co-precipitation Synthesis Method for Protein Separation."

Sulistyaningsih, T., Juari Santosa, S., Siswanta, D., Rusdiarso, B., 2015. Synthesis and Characterization of Magnetites Obtained from Mechanically and Sonochemically Assisted Coprecipitation and Reverse Co-precipitation Methods. Int. J. Mater. Mech. Manuf.

Hariani, P.L., Faizal, M., Ridwan, R., Marsi, M., Setiabudidaya, D., Jan 2013. Synthesis and Properties of $Fe_3O_4$ Nanoparticles by Co-precipitation Method to Removal Procion Dye. Int. J. Environ. Sci. Dev. 4 (3), 2013.

S. N. A. Bahrain, N. M. Sarah, and S. Mohamad, "Novel functionalized polythiophene-coated Fe3O4 nanoparticles for magnetic solid-phase extraction of phthalates," Polymers (Basel)., 4, no 3, 2016.

Wang, T., Wang, H., Chi, X., Li, R., Wang, J., 2014. Synthesis and microwave absorption properties of Fe-C nanofibers by electrospinning with disperse Fe nanoparticles parceled by carbon. Carbon N. Y. 74, 312–318.

G. Qiu, Q. Wang, and M. Nie, "Polypyrrole-Fe3O4 Magnetic Nanocomposite Prepared by Ultrasonic Irradiation," pp. 68–74, 2006.

Tang, S. et al, 2011. "Polymerization of aniline under various concentrations of APS and. HCl" 43 (8), 667–675.

P. Cao, J. D. Mangadlao, and R. C. Advincula,"Stimuli-Responsive Polymers and their Potential Applications in Oil-Gas Industry," no. August, 2015.

P. Li, C. Liu, Y. Song, X. Niu, H. Liu, and Y. Fan, "Influence of Fe3O4 Nanoparticles on the Preparation of Aligned PLGA Electrospun Fibers Induced by Magnetic Field," vol. 2013, 2013.

Iqbal, N., Wang, X., Babar, A.A., Zainab, G., Yu, J., Ding, B., 2017. Flexible $Fe_3O_4$@carbon nanofibers hierarchically assembled with $MnO_2$ particles for high- performance supercapacitor electrodes. Sci. Rep. 7 (1), 1–10.

B. J. Kim, S. G. Oh, M. G. Han, and S. S. I'm, "Synthesis and characterization of polyaniline nanoparticles in SDS micellar solutions," Synth. Met., vol. 122, no. 2, pp. 297–304, 2001

Qiu, G., Wang, Q., Nie, M., 2006. Polyaniline/$Fe_3O_4$ magnetic nanocomposite prepared by ultrasonic irradiation. J. Appl. Polym. Sci. 102 (3), 2107–2111.

Medeiros, E.S. et al, 2008. "Electrospun Nanofibers of Poly(vinyl alcohol). Reinforced with Cellulose Nanofibrils".

Lim, G.H., Choi, H.J., 2017. Fabrication of self-assembled polyaniline tubes and their electrorheological characteristics. Colloids Surfaces A 530 (May), 227–234.

Keivani, M.B., Zare, K., Aghaie, M., Aghaie, H., Monajjemi, M., Branch, N.T., 2010. "Synthesis of Nano Conducting Polymer-Based Polyaniline and it's Composite. Mechanical Properties, Conductivity and Thermal Studies" 7 (1), 105–110.

S. Wang, G. Xie, J. Zhang, S. Zhang, and T. Li, "Structure, thermal and luminescence properties of Eu/Tb(BA)3 phen/PAN fibres fabricated by electrospinning," vol. 78, pp. 445–451, 2018.

Sun, L., Zhan, L., Shi, Y., Chu, L., Ge, G., He, Z., 2014. Microemulsion synthesis and electromagnetic wave absorption properties of monodispersed $Fe_3O_4$/polyaniline core- shell nanocomposites. Synth. Met. 187, 102–107.